



Universiteit  
Leiden  
The Netherlands

## Discovery of selective diacylglycerol lipase $\beta$ inhibitors

Zhu, N.

### Citation

Zhu, N. (2024, May 22). *Discovery of selective diacylglycerol lipase  $\beta$  inhibitors*. Retrieved from <https://hdl.handle.net/1887/3754188>

Version: Publisher's Version

License: [Licence agreement concerning inclusion of doctoral thesis in the Institutional Repository of the University of Leiden](#)

Downloaded from: <https://hdl.handle.net/1887/3754188>

**Note:** To cite this publication please use the final published version (if applicable).

# Chapter 1

## General introduction

Zhu, N., Janssen, A.P.A. & van der Stelt, M. Understanding and Targeting the Endocannabinoid System with Activity-Based Protein Profiling. *Isr. J. Chem.* **63**, e202200115 (2023).

In 1995, Cravatt and colleagues reported the identification of a sleep-inducing lipid, oleamide (*N*-oleoylamine), which was isolated from the cerebrospinal fluid of sleep-deprived cats.<sup>1</sup> Oleamide was found to be rapidly hydrolyzed to oleic acid by an unidentified membrane-bound enzyme, whose activity was completely inhibited by phenylmethylsulfonyl fluoride (PMSF, **3**). They used this information to isolate the enzyme by making use of affinity beads modified with a covalent reversible inhibitor to purify the enzyme from rat liver plasma membranes, followed by amino acid sequencing and genomic analysis.<sup>2</sup> The enzyme identified was fatty-acid amide hydrolase (FAAH). FAAH also proved to be responsible for the hydrolysis of the amide bond of the endocannabinoid *N*-arachidonylethanolamine (AEA, anandamide)<sup>3</sup>, which is an endogenous agonist of the cannabinoid receptors type 1 and 2 (CB<sub>1</sub>R and CB<sub>2</sub>R). FAAH thereby effectively terminates the signaling of AEA. FAAH belongs to the enzyme family of serine hydrolases, which employ a catalytic serine residue to hydrolyze their substrates. A large number of serine hydrolases had been identified, but the biological function of many members was unknown due to the lack of specific chemical tools. Inhibitors containing fluorophosphonates (FP) were previously shown to be highly reactive to serine hydrolases.<sup>4,5</sup> Inspired by this observation, Cravatt and his team designed and synthesized FP-biotin, a broad-spectrum inhibitor containing a fluorophosphonate warhead and a biotin as reporter tag, thereby creating the very first activity-based probe (ABP), to study the activity of serine hydrolases in complex biological systems.<sup>6</sup> FP-biotin labeled FAAH as well as other serine hydrolases in an activity-dependent manner in cell and tissue lysates by covalent binding to the nucleophilic serine residue. This seminal paper can be considered the foundation of activity-based protein profiling (ABPP) for the identification and investigation of the metabolic enzymes and their inhibitors. In follow-up studies, an avidin-based isolation method was generated which enabled the rapid and simultaneous identification of multiple FP-biotinylated serine hydrolases after trypsin digestion and mass spectrometry (MS) analysis.<sup>7,8</sup> These early papers showed the potential of ABPP for the efficient discovery and profiling of inhibitors for serine hydrolases. In this Chapter, we will focus on the role of ABPP in the discovery of inhibitors for the biosynthesis and metabolism of ana and 2-arachidonoylglycerol (2-AG), another endogenous agonist of CB<sub>1</sub>R and CB<sub>2</sub>R. We will discuss the biological effects of the inhibitors in disease models and their therapeutic applications, but first we will start with a brief introduction of the endocannabinoid system (ECS).

## 1.1 The endocannabinoid system

AEA and 2-AG are the two main endocannabinoids that activate CB<sub>1</sub>R and CB<sub>2</sub>R to modulate various biological processes, such as neurotransmission, synaptic plasticity, memory formation and learning, locomotion, mood, pain sensation and immune response.<sup>9,10</sup> Both endocannabinoids are produced ‘on demand’ from membrane phospholipids and rapidly inactivated by metabolic enzymes after actions.<sup>11</sup> The biosynthesis and metabolism of each endocannabinoid is mediated by multiple enzymes (Figure 1.1).<sup>12</sup> The endocannabinoids, their biosynthetic and metabolic enzymes and cannabinoid receptors constitute the ECS. In the first step of AEA biosynthesis, phospholipase A2 group IVE (PLA2G4E)<sup>13</sup> or phospholipase A1/2

acyltransferase 1-5 (PLAAT1-5)<sup>14</sup> transfer the arachidonoyl moiety at the *sn*1 position from phosphatidylcholine (PC) to phosphatidylethanolamine (PE) to form *N*-arachidonoyl-phosphatidylethanolamine. PLA2G4E is a Ca<sup>2+</sup>-dependent serine hydrolase, whereas PLAAT1-5 are cysteine hydrolases. Subsequently, *N*-arachidonoyl-phosphatidylethanolamine is hydrolyzed to AEA by *N*-acylphosphatidylethanolamine phospholipase D (NAPE-PLD)<sup>15</sup> in one step or by the combined actions of other enzymes, including  $\alpha/\beta$ -hydrolase domain-containing 4 (ABHD4)<sup>16</sup>, GDE1<sup>17</sup>, GDE4<sup>18</sup> or GDE7.<sup>19</sup> AEA is degraded to arachidonic acid (AA) and ethanolamine by FAAH<sup>2</sup> and to minor extent by *N*-acylethanolamine acid amidase (NAAA).<sup>20</sup> The biosynthesis of 2-AG from phosphatidylinositol-4,5-bisphosphate (PIP<sub>2</sub>) is mediated by the consecutive actions of phospholipase C- $\beta$  (PLC $\beta$ ) and *sn*-1 specific diacylglycerol lipase  $\alpha$  and  $\beta$  (DAGLs).<sup>21</sup> 2-AG is metabolized to AA and glycerol, predominantly by monoacylglycerol lipase (MAGL) and to a lesser extent by ABHD6 and ABHD12.<sup>22</sup> Inhibitors are required to study the biological effects of these enzymes in an acute and spatiotemporal manner. In the sections below, we will discuss how ABPP enabled the discovery of highly potent and selective inhibitors for the ECS enzymes.

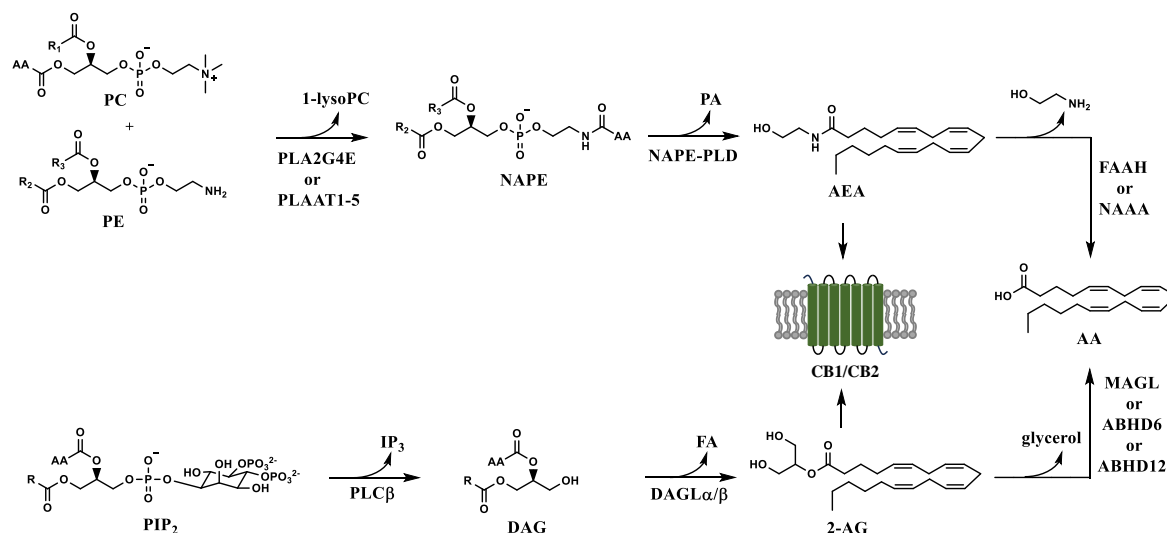


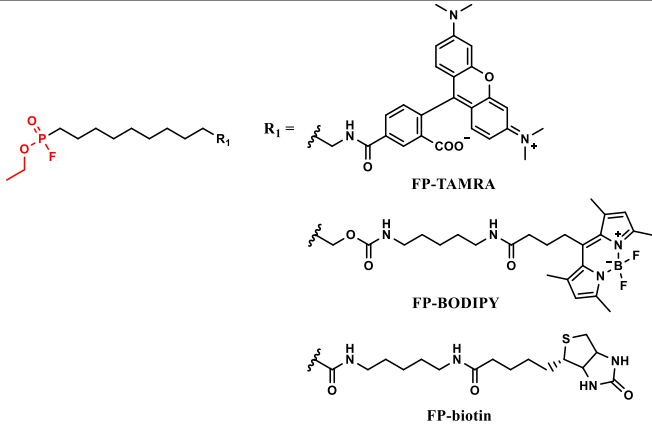
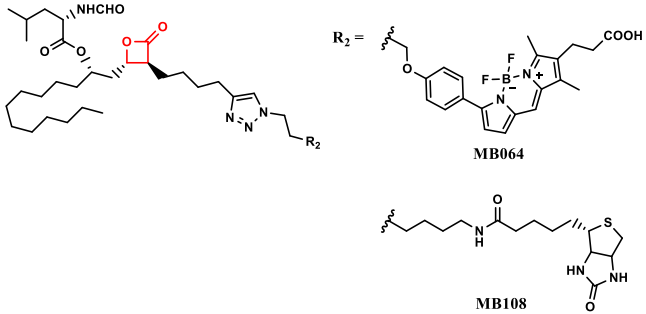
**Figure 1.1** Overview of major metabolic pathways of the endocannabinoids AEA and 2-AG that activate the cannabinoid receptors type 1 and 2. PLA2G4E or PLAAT1-5 transfer the arachidonoyl group from PC to the amine of PE to produce NAPEs, which are subsequently hydrolyzed mainly by NAPE-PLD to form AEA. AEA is metabolized by FAAH and to minor extent by NAAA to AA and ethanolamine. PLC $\beta$  converts PIP<sub>2</sub> to diacylglycerol (DAG). DAG is hydrolyzed by DAGLs to 2-AG, which is in turn degraded by MAGL, ABHD6 or ABHD12. PLA2G4E, FAAH, DAGLs, MAGL, ABHD6 and ABHD12 are serine hydrolases.

## 1.2 Development of broad-spectrum ABPs for ECS enzymes

ABPs can be classified into two categories: broad-spectrum ABPs and tailored ABPs.<sup>23</sup> Broad-spectrum ABPs enable target identification and parallel profiling of protein families to evaluate potency and selectivity of inhibitors. Tailored ABPs, based on specific inhibitors, are ideal for identifying potential off-targets *in situ* and *in vivo*, visualizing and evaluating the localization of proteins in cells, tissues and organisms. Two types of broad-spectrum ABPs have been

developed to study serine hydrolases, i.e. FP-based probes<sup>6,24</sup> and  $\beta$ -lactone-based probes<sup>25,26</sup> (Table 1.1).

**Table 1.1** Overview of broad-spectrum activity-based probes (ABPs) for ECS enzymes.

Chemotype	Probe	Structure	Labeling profile
Fluorophosphonates (FP)	FP-based probes	 <p>FP-TAMRA</p> <p>FP-BODIPY</p> <p>FP-biotin</p>	Serine hydrolases, including FAAH, MAGL, DAGL $\alpha$ , DAGL $\beta$ , ABHD6, ABHD12, PLA2G4E, CES enzymes
$\beta$ -lactones	$\beta$ -lactone-based probes	 <p>MB064</p> <p>MB108</p>	Serine and cysteine hydrolases, including DAGL $\alpha/\beta$ , ABHD6, ABHD12, ABHD16a, DDHD2, PLAATs

As discussed in the introduction, FP-TAMRA<sup>24</sup> (also known as FP-rhodamine) and FP-biotin<sup>6</sup> label multiple serine hydrolases of the ECS, such as FAAH, MAGL, DAGL $\alpha$ , DAGL $\beta$ , ABHD6 and ABHD12. This allowed assessment of ECS inhibitor activity and selectivity in cells and brain proteomes. For example, oleoyl trifluoromethyl ketone (TFMK, **2**) was revealed to react with multiple brain membrane serine hydrolases by ABPP with FP-biotin.<sup>7</sup> By combining ABPP with targeted lipidomics, MAGL was demonstrated to be the most prominent 2-AG hydrolase in mouse brain followed by ABHD12 and ABHD6, accounting for ~85%, ~9% and ~4% of the total hydrolase activity respectively.<sup>22</sup> In addition, PLA2G4E was identified by using FP-biotin as the canonical *N*-acetyltransferase (NAT), which is responsible for the Ca<sup>2+</sup>-dependent formation of NAPes.<sup>13</sup> To extend the chemical toolbox for serine hydrolases, Janssen *et al.* synthesized and characterized a new fluorescent FP-probe, FP-BODIPY.<sup>27</sup> Despite containing the same FP warhead, FP-BODIPY was able to label different serine hydrolases in mouse brain lysate compared to FP-TAMRA, which may be due to its higher lipophilicity. This would promote its interaction with membrane proteins resulting in enhanced labeling of several membrane-bound serine hydrolases including DAGL $\alpha$ .

Next to FP-based probes,  $\beta$ -lactone-based probes MB064<sup>25</sup> and MB108<sup>26</sup>, have been used to label serine hydrolases of the ECS. These probes were based on tetrahydrolipstatin (THL, Orlistat, **1**), which is an FDA-approved drug for the treatment of obesity and was initially reported to covalently inhibit pancreatic and gastric lipases.<sup>28–30</sup> In 2003, Bisogno *et al.* reported the identification of DAGL $\alpha$  and DAGL $\beta$  and found that they were potently inhibited by THL.<sup>21</sup> A series of THL derivatives was synthesized and investigated as DAGL inhibitors, which led to the discovery of OMDM-188.<sup>31</sup> Biochemical assays using radiolabeled natural substrates showed good selectivity of OMDM-188 for DAGL over FAAH and MAGL. However, competitive ABPP studies for THL and OMDM-188 were unavailable at that time due to the lack of broad-spectrum ABPs targeting DAGL $\alpha$ . To develop ABPs for DAGL $\alpha$ , Baggelaar *et al.* designed a fluorescent probe MB064<sup>25</sup> and a biotinylated probe MB108.<sup>26</sup> These  $\beta$ -lactone-based probes have a more restricted labeling profile in comparison with FP-based probes and they were proven to label the serine hydrolases ABHD6, ABHD12 and cysteine hydrolases PLAATs.<sup>32</sup> The selectivity of THL and OMDM-188 was evaluated in ABPP studies by using these probes and the results revealed their cross reactivity to several ABHD enzymes and phospholipase DDHD2. A probe cocktail of MB064 and FP-BODIPY was developed to visualize most ECS enzymes in tissue samples in a single experiment, which promoted the efficiency of selectivity assessments.<sup>27</sup> A combination of MB108 and FP-biotin was employed in label-free quantitative proteomics to assess the protein interaction landscape of DAGL inhibitor DH376 in diverse organs.<sup>33</sup>

### 1.3 Development of selective inhibitors and tailored ABPs for ECS enzymes

Early serine hydrolase inhibitors, such as THL (**1**), TFMK (**2**), PMSF (**3**) and RHC80267 (**4**), lacked selectivity required for *in vivo* investigation of FAAH, MAGL and DAGL (Figure 1.2). The discovery of highly potent and selective inhibitors has benefited greatly from the application of ABPP. Numerous inhibitors for ECS enzymes have been reported and most of them can be classified into 3 main chemotypes:  $\alpha$ -ketoheterocycles, carbamates and ureas. There are also specific chemotypes for several ECS enzymes, such as glycine sulfonamides for DAGLs, thioureas for ABHD12,  $\alpha$ -ketoamides for PLAATs, and pyrimidine-4-carboxamides for NAPE-PLD. In addition, various tailored ABPs have been developed based on selective inhibitors, which were used to study their selectivity across the entire proteome *in situ* and *in vivo* and to visualize target activity in cells and intact tissues. In the following sections we will discuss the various inhibitor chemotypes profiled with ABPP.

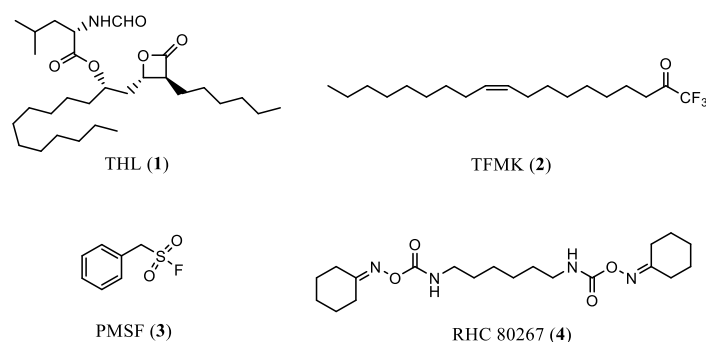


**Figure 1.2** Non-selective serine hydrolase inhibitors.

### 1.3.1 $\alpha$ -ketoheterocycle-based inhibitors for FAAH and DAGL

$\alpha$ -ketoheterocycles were initially disclosed by Edwards *et al.* as effective protease inhibitors.<sup>34</sup> The electrophilic carbonyl of  $\alpha$ -ketoheterocycles reversibly reacts with the catalytic serine to form a hemiketal intermediate. Boger *et al.* reported the development of  $\alpha$ -ketoheterocycles as highly active FAAH inhibitors in 2000 (Figure 1.3).<sup>35</sup> Leung *et al.* employed ABPP with FP-based probes to assess both potency and selectivity of this chemotype for multiple serine hydrolases and identified two off-targets, namely triacylglycerol hydrolase (TGH) and neutral cholesterol ester hydrolase 1 (KIAA1363).<sup>8</sup> Structure-activity relationship (SAR) studies for  $\alpha$ -ketoheterocycles afforded OL-135 (**5**) as a potent FAAH inhibitor with nanomolar activity and excellent selectivity over TGH (>10000-fold) and KIAA1363 (300-fold).<sup>36</sup> Moreover, OL-135 elevated brain AEA levels and promoted CB2-dependent analgesia in spinal nerve ligation model of neuropathic pain.<sup>37</sup> However, OL-135 showed a relatively short *in vivo* duration of action. Structural studies of FAAH with OL-135 derivatives<sup>38–40</sup> revealed that the adjacent Cys269 could be covalently and irreversibly trapped by a cysteine warhead to improve potency and *in vivo* half-life. Therefore, a series of OL-135 analogues (*e.g.* **6**) with different types of cysteine-targeted warheads were developed.<sup>41,42</sup> ABPP studies showed that the most promising compounds exhibited higher potency than OL-135 and good selectivity for FAAH over TGH, KIAA1363, MAGL and ABHD6. Moreover, these compounds increased brain *N*-acylethanolamine (NAE) levels and exhibited sustained (> 6 h) antinociceptive activity in a model of neuropathic pain.<sup>42</sup>

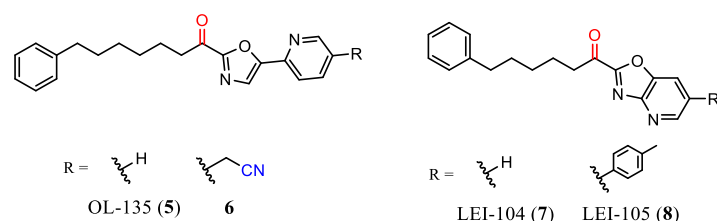


**Figure 1.3** Covalent reversible FAAH and DAGL inhibitors based on  $\alpha$ -ketoheterocycle warhead.

Using pharmacophore models, Baggelaar *et al.* discovered an  $\alpha$ -ketoheterocycle compound, LEI-104 (**7**), an OL-135 analogue, as the first covalent reversible inhibitor for

DAGL $\alpha$ .<sup>25</sup> Competitive ABPP using MB064 and FP-TAMRA confirmed FAAH as an off-target of LEI-104. Screening a large focused library (>1000 compounds) of  $\alpha$ -ketoheterocycles established the SAR.<sup>43</sup> Structure-guided design led to the development of LEI-105 (**8**) as a highly potent inhibitor for DAGL $\alpha$  and DAGL $\beta$ .<sup>26</sup> Competitive ABPP using  $\beta$ -lactone-based probes and FP-based probes indicated that LEI-105 was more selective than LEI-104, because it did not target FAAH or any other serine hydrolase. Biological studies showed that LEI-105 dose-dependently decreased 2-AG levels without modulating AEA levels in Neuro2A cells. LEI-105 treatment significantly suppressed depolarization-induced suppression of inhibition (DSI) in mouse hippocampal slices, thereby confirming the ‘on demand’ model<sup>11</sup> of endocannabinoid production.

### 1.3.2 Carbamate-based inhibitors for FAAH and MAGL

Another frequently encountered chemotype in serine hydrolase inhibitors are the carbamates. For example, URB597 (**9**), based on *O*-aryl carbamate, was reported as a potent, selective and *in vivo* active FAAH inhibitor in 2003 (Figure 1.4B).<sup>44</sup> *In vivo* studies showed that administration of URB597 elevated brain AEA levels without modifying 2-AG levels and exerted anti-nociceptive and anxiolytic effects in animal models. Kinetics and dialysis studies indicated the irreversible interaction of URB597 with FAAH, possibly via its active serine residue. Alexander and Cravatt confirmed the carbamylation of the catalytic residue Ser241 using MS analysis (Figure 1.4A).<sup>45</sup> To directly identify *in vivo* targets of FAAH-directed carbamates, a click-chemistry probe JP104 (**10**) was synthesized and employed.

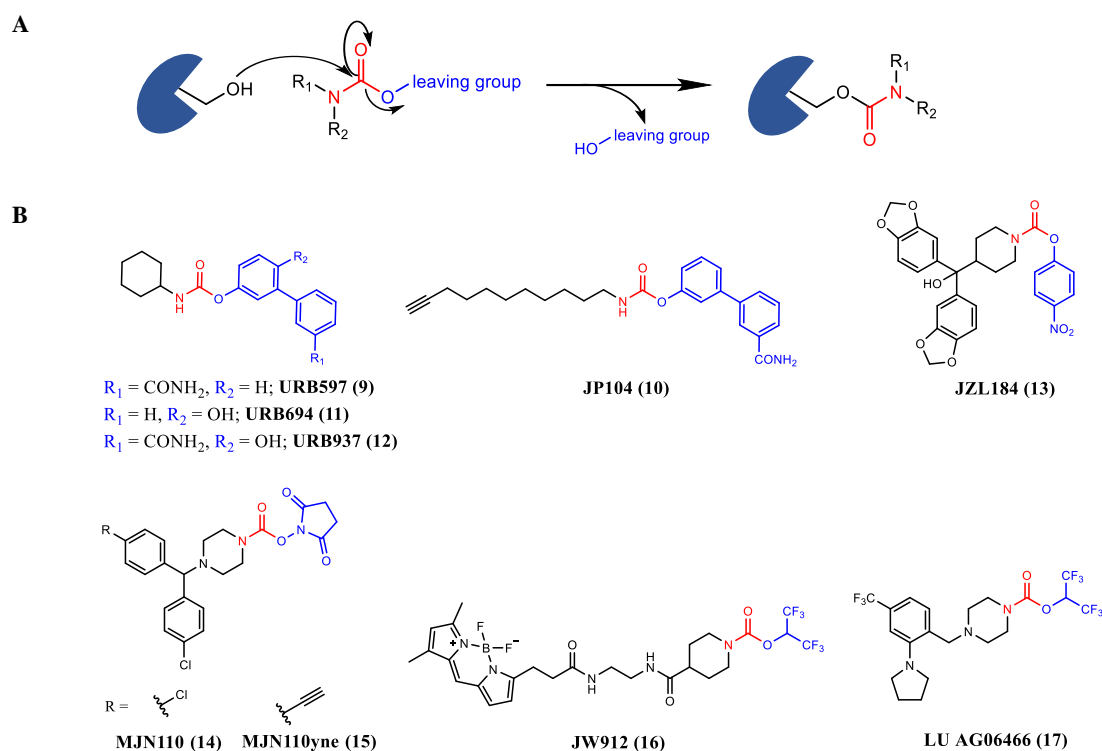


**Figure 1.4** (A) Mechanism of carbamate-based serine hydrolases inhibitors. (B) Covalent irreversible inhibitors and probes based on carbamates targeting MAGL and FAAH.



ABPP studies identified FAAH as the primary target of JP104 in brain. Several carboxylesterases (CES) were identified enzymes as the off-targets in peripheral organs.<sup>45,46</sup> To improve selectivity and *in vivo* stability, a second generation of carbamate-based FAAH inhibitors was developed.<sup>47</sup> The representative compound URB694 (**11**) showed attenuated activity to CES enzymes and improved *in vivo* metabolic stability. URB937 (**12**) was peripherally restricted and exhibited antinociceptive effects in rat models of peripheral nerve injury and inflammation.<sup>48,49</sup>

In an extensive competitive ABPP screening of carbamate-based compounds, WWL98 was identified as an inhibitor for several serine hydrolases, including FAAH, MAGL and ABHD6.<sup>50</sup> SAR studies led to the development of JZL184 (**13**) as a potent, selective and brain active MAGL inhibitor.<sup>51</sup> *In vitro* and *in vivo* ABPP studies indicated the selectivity of JZL184 for MAGL over ~40 other serine hydrolases. JZL184 dose-dependently elevated 2-AG levels and reduced AA levels in the brain. JZL184 exhibited selectivity across different tissues, but it showed tissue-dependent effects on monoacylglycerols (MAGs) and AA levels.<sup>52</sup> These results indicated a more general metabolic function of MAGL. Of note, JZL184 was shown to inhibit CES in the periphery and to elevate AEA levels by inhibiting FAAH in chronic and high-dosing treatments.<sup>52–54</sup> In subsequent studies, the effect of the carbamate leaving group on MAGL inhibitory potency and selectivity was studied, leading to the development of KML29. This compound, with a hexafluoroisopropanol (HFIP) leaving group, exhibited good potency and improved selectivity over FAAH and CES.<sup>54</sup> Modification of KML29 on the staying group resulted in JW651, which was highly active and selective for MAGL with ABHD6 as the only identified off-target at high concentrations.<sup>55</sup> Substituting the HFIP moiety in JW651 with an *N*-hydroxysuccinimidyl (NHS) afforded inhibitor MJN110 (**14**). To identify potential off-targets alkynylated analogues JW651yne and MJN110yne (**15**) were developed. Competitive ABPP studies indicated that both inhibitors were highly selective across the entire proteome. Probe JW912 (**16**), containing an HFIP carbamate warhead and a BODIPY fluorophore, was developed for *in situ* labeling and visualization of MAGL and ABHD6.<sup>55</sup> JW912 selectively labeled MAGL in H29 cells and ABHD6 in Neuro2A cells. The activity of the probe was blocked by MAGL inhibitor JW651 and ABHD6 inhibitor KT195, respectively. Based on JW651, another fluorescent probe DH463 was developed and used to visualize and quantify MAGL activity in cells at the nanoscale level by using PharmacoSTORM, a super-resolution imaging method.<sup>56</sup> Application of FP-TAMRA and JW912 enabled the simultaneous optimization of potency and selectivity of MAGL inhibitors in a medicinal chemistry program, which led to the discovery of Lu AG06466 (previously ABX-1431, **17**) as a highly potent, selective and orally available MAGL inhibitor.<sup>57</sup> A single dose of Lu AG06466 was well-tolerated and showed a positive effect for patients with Tourette syndrome in a phase 1b study.<sup>58</sup> However, it failed in a phase 2 clinical trial for Tourette syndrome.<sup>59</sup> Pfizer also disclosed a series of carbamate-based MAGL inhibitors with PF-06795071 as a representative compound containing a [3.1.0] pyrazole core system and a trifluoromethyl glycol leaving group.<sup>60</sup> PF-06795071 exhibited comparable potency and selectivity to inhibitors containing the HFIP leaving group but significantly increased solubility. PF-06795071 elevated brain 2-AG levels with a concomitant reduction in the levels of AA and inflammatory markers PGE<sub>2</sub>, IL-1 $\beta$  and

TNF- $\alpha$ . No clinical trial studies have been reported for PF-06795071 to date.

### 1.3.3 Urea-based inhibitors for FAAH, DAGL and ABHD6

The tetrazole urea LY2183240 was initially reported as an AEA reuptake inhibitor<sup>61</sup>, but its mechanism-of-action was later shown to be dependent on the carbamylation of FAAH's catalytic serine residue and releasing the tetrazole moiety.<sup>62</sup> In 2009, benzothiophene piperazine and piperidine ureas were reported as selective FAAH inhibitors and some of them showed anti-hyperalgesic effects in a rat model of inflammatory pain.<sup>63</sup> Janssen and Pfizer disclosed several urea-based compounds as FAAH inhibitors.<sup>64–66</sup> JNJ-42165279 (**18**) was highly potent and selective and exhibited beneficial effects in rat models of neuropathic pain and inflammation (Figure 1.5).<sup>67</sup> JNJ-42165279 was well-tolerated in both single and multiple-ascending dose clinical studies.<sup>68,69</sup> JNJ-42165279 (25 mg daily) elicited a moderate anxiolytic effect in subjects with social anxiety disorder and a greater effect was observed in individuals with more complete inhibition of FAAH.<sup>70</sup> JNJ-42165279 is currently under investigation for the treatment of post-traumatic stress disorder (PTSD) at a dose of 25 mg twice daily. PF-04457845 (**19**) was originally developed for treatment of osteoarthritis pain, but failed in phase 2 clinical trials due to a lack of efficacy.<sup>71</sup> In a phase 2a study of cannabis use disorder, PF-04457845 reduced symptoms of cannabis withdrawal and self-reported cannabis use in men.<sup>72</sup> PF-04457845 was also reported to enhance the recall of fear extinction but not to influence within-session fear extinction.<sup>73</sup>

In 2016, one healthy volunteer who received 50 mg per day of the FAAH inhibitor BIA 10-2474 (**20**) died in a phase 1 clinical trial due to brain damage.<sup>74</sup> Another five participants who received the same dose were hospitalized. This tragedy resulted in the halt of all clinical trials with FAAH inhibitors. Off-target activities of BIA 10-2474 and/or its metabolites were hypothesized to be the cause of the serious adverse events. Van Esbroeck *et al.* employed gel-based and MS-based ABPP with FP-based probes and  $\beta$ -lactone-based probes to reveal the protein interaction landscape of BIA 10-2474.<sup>75</sup> ABPP studies in human cells and human brain revealed numerous off-targets of BIA 10-2474, including FAAH2, ABHD6, ABHD11, LIPE, CTSA, PLA2G15, PNPLA6 and CES. In contrast, PF-04457845, taken along as a safe control compound, displayed good selectivity. Many of the off-targets regulate lipid metabolism. Lipidomic analysis confirmed that BIA 10-2474 altered the levels of NAEs and several other lipid classes, whereas PF-04457845 predominantly elevated the levels of NAEs. This study highlighted the application of ABPP as a versatile method to assess on-target engagement and off-target activities of covalent drugs to guide drug discovery and development processes.

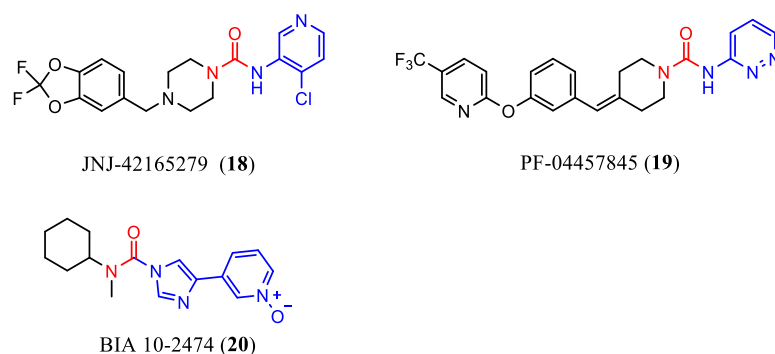


**Figure 1.5** Clinical FAAH inhibitors based on a urea scaffold.

Urea-based compounds, especially 1,2,3-triazole ureas, are widely investigated as DAGL inhibitors (Figure 1.6). Initially, KT117 (**21**) was identified to inhibit DAGL $\beta$  in an ABPP-based screening of a library of thirty 1,2,3-triazole ureas by using FP-TAMRA.<sup>76</sup> KT116 (**22**), a 1,4-regioisomer, was 10-fold more potent than the 2,4-regioisomer KT117. However, KT116 inhibited several other serine hydrolases, including FAAH, MAGL, ABHD6, ABHD11 and PLA2G7. Lead optimization led to the discovery of two DAGL inhibitors KT109 and KT172 (**23** and **24**). Competitive ABPP studies identified ABHD6 as the common off-target of both KT109 and KT172. DAGL-tailored probe HT-01 (**25**) was generated from these 1,2,3-triazole ureas. Competitive ABPP with HT-01 using recombinant DAGLs indicated that KT109 and KT172 were 55-fold and 2-fold selective for DAGL $\beta$  over DAGL $\alpha$ , respectively. However, KT109 was reported to inhibit DAGL $\alpha$  with high potency in other assays.<sup>77,78</sup> KT109 and KT172, but not ABHD6 inhibitor KT195 (**26**), reduced the levels of 2-AG, AA, and prostaglandin E2 and D2 (PGE<sub>2</sub> and PGD<sub>2</sub>) in macrophages and suppressed the production of proinflammatory cytokine TNF $\alpha$  in LPS-treated mice. Using KT109 as a starting point, DH376 and DO34 (**27** and **28**) were developed as highly potent, and centrally active dual DAGL inhibitors.<sup>78,79</sup> DH376 is a 2,4-substituted 1,2,3-triazole urea, which was shown to have a higher binding affinity for DAGL $\alpha$  than its 1,4-substituted isomer in a structure-kinetics relationship study.<sup>80</sup> Via a click reaction between the alkyne of DH376 and the azide of a BODIPY-based fluorophore, DH379 (**29**) was generated as another DAGL-tailored probe. DH379 labeled both DAGL $\alpha$  and DAGL $\beta$  in mouse brain. ABPP studies with FP-based probes, HT-01 and DH379 revealed that DH376 and DO34 dose-dependently inhibited DAGLs *in vitro* and *in vivo* with cross reactivity to ABHD6 and CES1C for both inhibitors. In addition, DO34 also inhibited PLA2G7, ABHD2, and PAFAH2. In contrast, DO53 (**30**), a control compound derived from KT195, inhibited all off-targets without affecting DAGLs activity. Interestingly, DAGL $\alpha$  was revealed to have a short *in vivo* half-life of 2-4 h, which indicated a tight regulation of 2-AG levels by DAGL protein synthesis and breakdown. Acute blockade of DAGL by DH376 and DO34, but not by DO53, elevated 1-stearoyl-2-arachidonoyl-*sn*-glycerol (SAG) levels and reduced the levels of 2-AG, AEA, AA, PGE<sub>2</sub> and PGD<sub>2</sub>. The reduction in AEA levels might suggest an *in vivo* crosstalk of AEA and 2-AG. Moreover, both inhibitors completely blocked cerebellar GABAergic (DSI) and hippocampal glutamatergic (DSE) neurotransmissions and attenuated LPS-induced neuroinflammation.

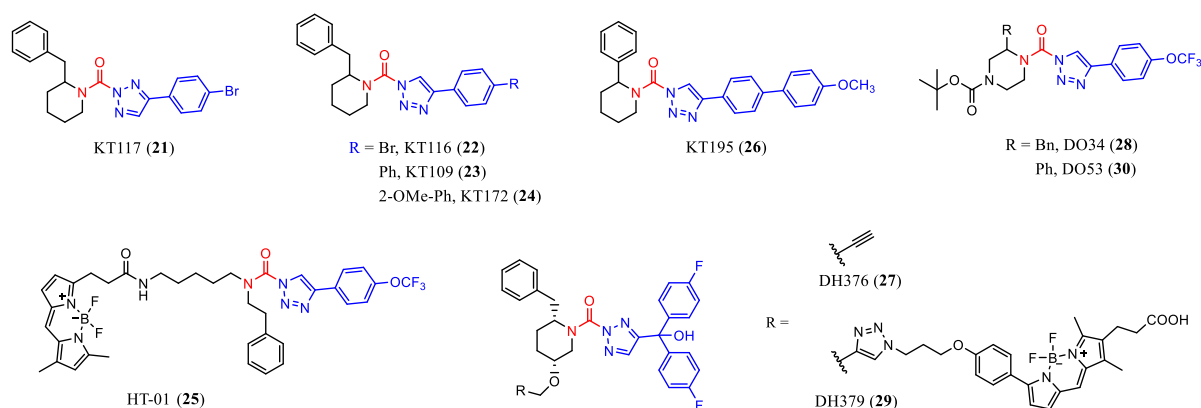


**Figure 1.6** DAGL inhibitors and probes, and control compounds based on 1,2,3-triazole ureas.

KT195 was initially developed as a control compound to address the selectivity problem of KT109 and KT172, but proved to be a good ABHD6 inhibitor. Further SAR studies led to the development of KT182 (as a systemic inhibitor), KT203 (as a peripherally restricted inhibitor), and KT185 (as an orally active inhibitor).<sup>81</sup> Competitive ABPP with FP-TAMRA and HT-01 revealed that these three compounds were potent ABHD6 inhibitors and selective up to 1  $\mu$ M. *In vivo* ABPP studies confirmed the high potency and selectivity of these inhibitors in brain and liver. KT182 was recently evaluated in rodent models of multiple sclerosis (MS), but showed limited efficacy.<sup>82,83</sup>

### 1.3.4 Specific chemotypes

#### 1.3.4.1 Glycine sulfonamides for DAGL

Glycine sulfonamides (Figure 1.7) were identified as non-covalent DAGL inhibitors in a high-throughput screening (HTS) by researchers from Bristol-Myers Squibb.<sup>84</sup> SAR studies by Janssen *et al.* led to the development of LEI-106 (**31**) as a DAGL $\alpha$  inhibitor with good potency.<sup>85</sup> Gel-based ABPP with FP-TAMRA and MB064 identified ABHD6 as the off-target of LEI-106, which was further confirmed by the biochemical ABHD6 activity assay. In 2016, another extensive SAR study of glycine sulfonamides was published, in which several compounds were developed as highly potent, peripherally restricted and orally available DAGL inhibitors.<sup>86</sup>

#### 1.3.4.2 Thioureas for ABHD12

Due to the limited cross-reactivity of ABHD12 to previously described inhibitors, novel chemotypes of ABHD12 inhibitors were needed. To this end, an enzyme-coupled assay for ABHD12 was used in a HTS, which led to the identification of a thiourea-based compound DO130 as a novel ABHD12 inhibitor.<sup>87</sup> To optimize this chemotype, JJH350<sup>88</sup>, a tailored ABP, originating from an *N*-hydroxyhydantoin (NHH) carbamate, was employed in competitive ABPP studies to evaluate the potency of the compounds. After a series of modifications,

compound DO264 (**32**) was discovered as a highly potent ABHD12 inhibitor. Competitive ABPP studies with FP-based probes and JJH350 revealed the excellent selectivity of DO264 for ABHD12 over other serine hydrolases in either *in vitro* or *in vivo* models. DO264 elevated lyso-PS and 20:4 PS as well as the cytokines TNF- $\alpha$ , IL-1 $\beta$ , and chemokines CCL3 and CCL4 levels in human monocytic cells.<sup>87,89</sup> Moreover, chronic treatment of DO264 significantly increased lyso-PS and 20:4 PS contents and heightened immunopathological responses to CLMV clone 13 (CI13) infection in mice, which indicated an immunosuppressive function of ABHD12. In a screening of serine hydrolase inhibitors for potentiating ferroptosis, ABHD12 inhibitor DO264 was found to enhance ferroptosis death caused by a lipid peroxidase GPX4 inhibitor RSL1.<sup>90</sup>

#### 1.3.4.3 $\alpha$ -ketoamides for PLAATs

Recently, it was discovered that  $\beta$ -lactone probe MB064 not only labeled serine hydrolases, but also several cysteine hydrolases, including PLAATs.<sup>32</sup> Using competitive ABPP with MB064, an  $\alpha$ -ketoamide derivative was identified as a PLA2G16 (also known as PLAAT3) inhibitor in a screening of 50 lipase inhibitors. Hit optimization led to the development of LEI-110 as a potent pan-PLAAT inhibitor. ABPP studies with FP-based probes and  $\beta$ -lactone-based probes revealed the high selectivity of LEI-110 for PLAATs over other enzymes in mouse brain membrane and cytosol proteomes. Further SAR studies led to the development of LEI-301 (**33**) as a selective pan-PLAAT inhibitor which was more potent than LEI-110.<sup>91</sup> LEI-301 exhibited a good selectivity profile within the ECS with minimal affinity for CB<sub>1</sub>R and CB<sub>2</sub>R and no inhibition for other enzymes, including FAAH, MAGL, ABHD6, PLA2G4E, NAPE-PLD, and DAGLs. Overexpression of PLAAT2 and PLAAT5 elevated NAEs levels in U2OS cells, which was reduced by LEI-301 treatment.

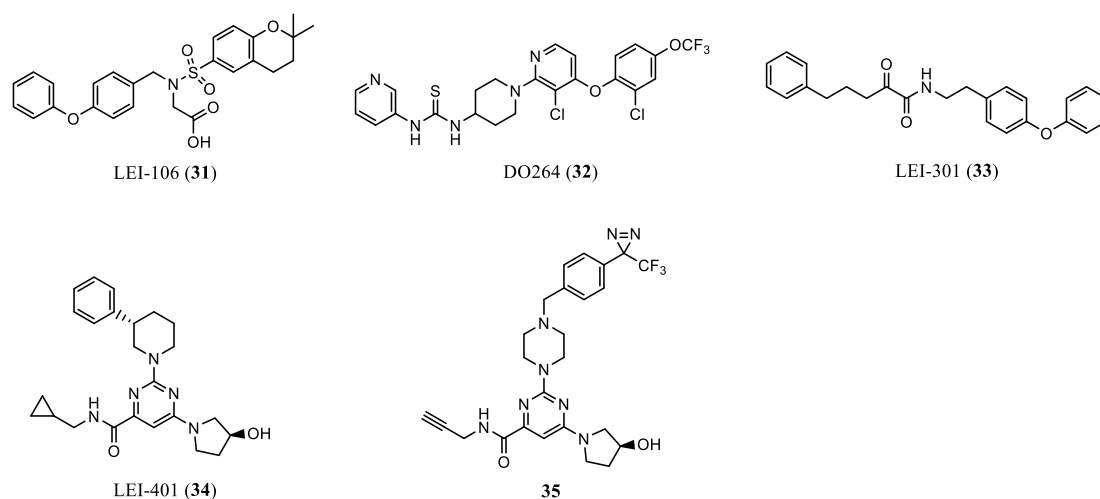


**Figure 1.7** Inhibitors and probes based on specific chemotypes.

#### 1.3.4.4 Pyrimidine-4-carboxamides for NAPE-PLD

NAPE-PLD is a metallo- $\beta$ -lactamase, which was identified as the principal enzyme producing NAEs in 2004.<sup>15</sup> Due to the lack of a catalytic serine or cysteine residue, NAPE-PLD cannot be targeted by previously described chemotypes. Recently, a pyrimidine-4-carboxamide was identified as a novel scaffold for NAPE-PLD inhibition in a HTS using a library of ~350,000 compounds.<sup>92,93</sup> Hit-to-lead optimization afforded compound LEI-401 (**34**), which showed good potency and selectivity for NAPE-PLD with no inhibitory activity for other metabolic enzymes in ECS. Based on LEI-401, a click-chemistry photoprobe (**35**) was synthesized containing a UV-active trifluoromethyl phenyl diazirine and an alkynyl handle. Affinity-based protein profiling (AfBPP) studies showed that recombinant NAPE-PLD could be labeled by the probe, which was concentration-dependently inhibited by LEI-401. In MS-based AfBPP studies, LEI-401 selectively inhibited NAPE-PLD without outcompeting other proteins labeled by the photoprobe. LEI-401 reduced mouse brain NAE levels in a NAPE-PLD dependent manner. Moreover, LEI-401 activated the hypothalamus–pituitary–adrenal (HPA) axis and reduced fear extinction, which were both reversed by the FAAH inhibitor URB597.<sup>44</sup>

## 1.4 Summary

Endocannabinoids are involved in various physiological functions and disease processes. The development of selective and *in vivo* active ABPs and inhibitors for ECS enzymes was a vital step to dissect the various endocannabinoid functions and established the therapeutic potential of these proteins. Various drug discovery strategies, such as HTS, structure-based design, and *de novo* design, have been employed to identify highly potent and selective inhibitors for ECS enzymes. ABPP efficiently guided the optimization of the hits by profiling their activity and selectivity in their native biological context. ABPP coupled with advanced imaging techniques such as PharmacOSTORM and CATCH<sup>94</sup> enables the visualization of enzymatic activity in tissue slices at nanometer resolution. Although FAAH and MAGL inhibitors have entered clinical studies, selective inhibitors are still lacking for PLA2G4E, DAGL $\alpha$  and DAGL $\beta$ . In addition, the enzymes involved in the alternative NAE biosynthesis routes are understudied. Selective inhibitors for these enzymes will be valuable for elucidating their biological functions. To conclude, ABPP is a valuable chemical biology technology that aids the design and evaluation of inhibitors. The combination of ABPP with advanced imaging technologies and lipidomics leads to a better understanding of physiological and pathological processes involving serine hydrolases. The generation of novel molecular therapies based on the ECS enzymes will certainly benefit from these advances.

## 1.5 Aim and outline of this thesis

Selective DAGL $\beta$  inhibitors are important for elucidating the physio(patho)logical functions of this enzyme and could be potential treatment of inflammation with reduced CNS side effects mediated by DAGL $\alpha$  inhibition. In view of this, the aim of the research described in this thesis is to develop DAGL $\beta$  selective inhibitors for evaluating the biological functions of DAGL $\beta$ .



In **Chapter 2**, an EnzChek lipase substrate assay for DAGL is optimized and miniaturized into a 384-well plate format to screen a library of 12,587 compounds using purified catalytic domain of DAGL $\beta$ . After the primary screening, confirmed screening, deselection, and dose-response evaluation, eight hits classified into four chemotypes are obtained. Hit **1** based on glycine sulfonamide, also known as LEI-106, exhibits the highest potency for DAGL $\beta$  and favorable physiological properties for hit optimization.

In **Chapter 3**, a comprehensive structure-activity relationship of glycine sulfonamides as DAGL inhibitors is explored through systematic modifications on different parts of this chemotype. While most of compounds discussed in this Chapter demonstrate comparable potency for both DAGL isoforms or slight selectivity for DAGL $\alpha$ , three compounds varying on the sulfonyl substituent display some selectivity for DAGL $\beta$ . This suggests the sulfonyl group as a modification hotspot for achieving selectivity for DAGL $\beta$ .

In **Chapter 4**, an in-depth structure-activity relationship study (SAR) is conducted to enhance DAGL $\beta$  selectivity, with a focus on optimizing the sulfonyl substituent of the glycine sulfonamide chemotype. This effort leads to the identification of 3,4-dihydro-2*H*-benzo[*b*][1,4]dioxepine as the optimal substituent on this position. Further optimization of potency and selectivity involves exploring other components of this chemotype, resulting in the discovery of six compounds with promising potency, selectivity and physiochemical properties. These findings position these compounds as the first-in-class DAGL $\beta$  selective inhibitors deserving further profiling and exploration.

In **Chapter 5**, a fluorescence-based plate reader assay using a GPCR activation-based endocannabinoid sensor (GRAB<sub>CB2.0</sub>) is established to assess the cellular activity of DAGL inhibitors. The sensor, expressed in mouse neuroblastoma cells (Neuro2A), demonstrates exquisite sensitivity to 2-AG and can be indirectly activated by adenosine triphosphate (ATP). In this assay, 23 DAGL inhibitors with diverse activities and isoform selectivities are evaluated. This profiling reveals that 2-AG production in Neuro2A upon ATP stimulation is primarily mediated by DAGL $\alpha$ .

In **Chapter 6**, representative DAGL $\beta$  selective inhibitors, **LEI-130** and **LEI-131**, along with a negative control compound, **LEI-132**, are profiled in *in vitro* and *in situ* studies. Mode-of-inhibition studies reveal a noncompetitive mechanism for LEI-130 and LEI-131 against DAGL $\beta$ , suggesting their binding to an allosteric pocket. *In vitro* and *in situ* ABPP studies of LEI-130 and LEI-131 confirm their activity against DAGL $\beta$  over a panel of proteins in mouse brain proteomes and living cells. Lipidomics analysis of LEI-130, LEI-131 and LEI-132 in N9 microglia and J774A.1 macrophage cells demonstrate that DAGL $\beta$  regulates the levels of 2-AG as well as its downstream lipids in a cell type-dependent manner. Furthermore, LEI-130, LEI-131 and LEI-132 all attenuate the LPS-stimulated cytokine production, suggesting the involvement of an unknown off-target in regulating this process.

In **Chapter 7**, the work presented in this thesis is summarized and new directions for future research are provided.

## Reference

1. Cravatt, B. F. *et al.* Chemical Characterization of a Family of Brain Lipids That Induce Sleep. *Science* **268**, 1506–1509 (1995).
2. Cravatt, B. F. *et al.* Molecular characterization of an enzyme that degrades neuromodulatory fatty-acid amides. *Nature* **384**, 83–87 (1996).
3. Devane, W. A. *et al.* Isolation and structure of a brain constituent that binds to the cannabinoid receptor. *Science* **258**, 1946–9 (1992).
4. Creighton, T. E. *Proteins: Structures and Molecular Properties*. W. H. Freeman (1992). doi:10.1002/jctb.280620121.
5. Christopher T. Walsh. *Enzymatic Reaction Mechanisms*. W. H. Freeman (1979). doi:10.1093/oso/9780195122589.001.0001.
6. Liu, Y., Patricelli, M. P. & Cravatt, B. F. Activity-based protein profiling: The serine hydrolases. *Proc. Natl. Acad. Sci. U.S.A.* **96**, 14694–14699 (1999).
7. Kidd, D., Liu, Y. & Cravatt, B. F. Profiling Serine Hydrolase Activities in Complex Proteomes. *Biochemistry* **40**, 4005–4015 (2001).
8. Leung, D., Hardouin, C., Boger, D. L. & Cravatt, B. F. Discovering potent and selective reversible inhibitors of enzymes in complex proteomes. *Nat. Biotechnol.* **21**, 687–691 (2003).
9. Baggelaar, M. P., Maccarrone, M. & van der Stelt, M. 2-Arachidonoylglycerol: A signaling lipid with manifold actions in the brain. *Prog. Lipid Res.* **71**, 1–17 (2018).
10. Mock, E. D., Gagestein, B. & van der Stelt, M. Anandamide and other N-acyl ethanolamines: A class of signaling lipids with therapeutic opportunities. *Prog. Lipid Res.* **89**, 101194 (2022).
11. Alger, B. E. & Kim, J. Supply and demand for endocannabinoids. *Trends Neurosci.* **34**, 304–315 (2011).
12. Punt, J. M., van der Vliet, D. & van der Stelt, M. Chemical Probes to Control and Visualize Lipid Metabolism in the Brain. *Acc. Chem. Res.* **55**, 3205–3217 (2022).
13. Ogura, Y., Parsons, W. H., Kamat, S. S. & Cravatt, B. F. A calcium-dependent acyltransferase that produces N-acyl phosphatidylethanolamines. *Nat. Chem. Biol.* **12**, 669–671 (2016).
14. Uyama, T. *et al.* Generation of N-Acylphosphatidylethanolamine by Members of the Phospholipase A/Acyltransferase (PLA/AT) Family. *J. Biol. Chem.* **287**, 31905–31919 (2012).
15. Okamoto, Y., Morishita, J., Tsuboi, K., Tonai, T. & Ueda, N. Molecular Characterization of a Phospholipase D Generating Anandamide and Its Congeners. *J. Biol. Chem.* **279**, 5298–5305 (2004).



16. Simon, G. M. & Cravatt, B. F. Endocannabinoid Biosynthesis Proceeding through Glycerophospho-N-acyl Ethanolamine and a Role for  $\alpha/\beta$ -Hydrolase 4 in This Pathway. *J. Biol. Chem.* **281**, 26465–26472 (2006).
17. Simon, G. M. & Cravatt, B. F. Anandamide Biosynthesis Catalyzed by the Phosphodiesterase GDE1 and Detection of Glycerophospho-N-acyl Ethanolamine Precursors in Mouse Brain. *J. Biol. Chem.* **283**, 9341–9349 (2008).
18. Tsuboi, K. *et al.* Glycerophosphodiesterase GDE4 as a novel lysophospholipase D: a possible involvement in bioactive N-acylethanolamine biosynthesis. *Biochim. Biophys. Acta, Mol. Cell Biol. Lipids* **1851**, 537–548 (2015).
19. Rahman, I. A. S. *et al.* Calcium-dependent generation of N-acylethanolamines and lysophosphatidic acids by glycerophosphodiesterase GDE7. *Biochim. Biophys. Acta, Mol. Cell Biol. Lipids* **1861**, 1881–1892 (2016).
20. Sun, Y.-X. *et al.* Involvement of N-acylethanolamine-hydrolyzing acid amidase in the degradation of anandamide and other N-acylethanolamines in macrophages. *Biochim. Biophys. Acta, Mol. Cell Biol. Lipids* **1736**, 211–220 (2005).
21. Bisogno, T. *et al.* Cloning of the first sn1-DAG lipases points to the spatial and temporal regulation of endocannabinoid signaling in the brain. *J. Cell Biol.* **163**, 463–468 (2003).
22. Blankman, J. L., Simon, G. M. & Cravatt, B. F. A Comprehensive Profile of Brain Enzymes that Hydrolyze the Endocannabinoid 2-Arachidonoylglycerol. *Chem. Biol.* **14**, 1347–1356 (2007).
23. Deng, H., Lei, Q., Wu, Y., He, Y. & Li, W. Activity-based protein profiling: Recent advances in medicinal chemistry. *Eur. J. Med. Chem.* **191**, 112151 (2020).
24. Patricelli, M. P., Giang, D. K., Stamp, L. M. & Burbaum, J. J. Direct visualization of serine hydrolase activities in complex proteomes using fluorescent active site-directed probes. *Proteomics* **1**, 1067–1071 (2001).
25. Baggelaar, M. P. *et al.* Inside Back Cover: Development of an Activity-Based Probe and In Silico Design Reveal Highly Selective Inhibitors for Diacylglycerol Lipase- $\alpha$  in Brain. *Angew. Chem. Int. Ed.* **52**, 12081–5 (2013).
26. Baggelaar, M. P. *et al.* Highly Selective, Reversible Inhibitor Identified by Comparative Chemoproteomics Modulates Diacylglycerol Lipase Activity in Neurons. *J. Am. Chem. Soc.* **137**, 8851–8857 (2015).
27. Janssen, A. P. A. *et al.* Development of a Multiplexed Activity-Based Protein Profiling Assay to Evaluate Activity of Endocannabinoid Hydrolase Inhibitors. *ACS Chem. Biol.* **13**, 2406–2413 (2018).
28. Hadvary, P., Lengsfeld, H. & Wolfer, H. Inhibition of pancreatic lipase *in vitro* by the covalent inhibitor tetrahydrolipstatin. *Biochem. J.* **256**, 357–361 (1988).
29. Hadvary, P., Sidler, W., Meister, W., Vetter, W. & Wolfer, H. The lipase inhibitor tetrahydrolipstatin binds covalently to the putative active site serine of pancreatic lipase. *J. Biol. Chem.* **266**, 2021–2027 (1991).

30. Gargouri, Y., Chahinian, H., Moreau, H., Ransac, S. & Verger, R. Inactivation of pancreatic and gastric lipases by THL and C12:0-TNB: a kinetic study with emulsified tributyrin. *Biochim. Biophys. Acta, Mol. Lipids Lipid Metab.* **1085**, 322–328 (1991).
31. Ortar, G. *et al.* Tetrahydrolipstatin Analogues as Modulators of Endocannabinoid 2-Arachidonoylglycerol Metabolism. *J. Med. Chem.* **51**, 6970–6979 (2008).
32. Zhou, J. *et al.* Activity-Based Protein Profiling Identifies  $\alpha$ -Ketoamides as Inhibitors for Phospholipase A2 Group XVI. *ACS Chem. Biol.* **14**, 164–169 (2019).
33. van Rooden, E. J. *et al.* Mapping in vivo target interaction profiles of covalent inhibitors using chemical proteomics with label-free quantification. *Nat. Protoc.* **13**, 752–767 (2018).
34. Edwards, P. D. *et al.* Design, synthesis, and kinetic evaluation of a unique class of elastase inhibitors, the peptidyl .alpha.-ketobenzoxazoles, and the x-ray crystal structure of the covalent complex between porcine pancreatic elastase and Ac-Ala-Pro-Val-2-benzoxazole. *J. Am. Chem. Soc.* **114**, 1854–1863 (1992).
35. Boger, D. L. *et al.* Exceptionally potent inhibitors of fatty acid amide hydrolase: The enzyme responsible for degradation of endogenous oleamide and anandamide. *Proc. Natl. Acad. Sci. U.S.A.* **97**, 5044–5049 (2000).
36. Boger, D. L. *et al.* Discovery of a Potent, Selective, and Efficacious Class of Reversible  $\alpha$ -Ketoheterocycle Inhibitors of Fatty Acid Amide Hydrolase Effective as Analgesics. *J. Med. Chem.* **48**, 1849–1856 (2005).
37. Chang, L. *et al.* Inhibition of fatty acid amide hydrolase produces analgesia by multiple mechanisms. *Br. J. Pharmacol.* **148**, 102–113 (2006).
38. Saghatelian, A. *et al.* Assignment of Endogenous Substrates to Enzymes by Global Metabolite Profiling. *Biochemistry* **43**, 14332–14339 (2004).
39. McKinney, M. K. & Cravatt, B. F. Structure-Based Design of a FAAH Variant That Discriminates between the N -Acyl Ethanolamine and Taurine Families of Signaling Lipids. *Biochemistry* **45**, 9016–9022 (2006).
40. Saghatelian, A., McKinney, M. K., Bandell, M., Patapoutian, A. & Cravatt, B. F. A FAAH-Regulated Class of N-Acyl Taurines That Activates TRP Ion Channels. *Biochemistry* **45**, 9007–9015 (2006).
41. Otrubova, K., Cravatt, B. F. & Boger, D. L. Design, Synthesis, and Characterization of  $\alpha$ -Ketoheterocycles That Additionally Target the Cytosolic Port Cys269 of Fatty Acid Amide Hydrolase. *J. Med. Chem.* **57**, 1079–1089 (2014).
42. Otrubova, K. *et al.* Rational Design of Fatty Acid Amide Hydrolase Inhibitors That Act by Covalently Bonding to Two Active Site Residues. *J. Am. Chem. Soc.* **135**, 6289–6299 (2013).
43. Janssen, F. J. *et al.* Comprehensive Analysis of Structure–Activity Relationships of  $\alpha$ -Ketoheterocycles as sn -1-Diacylglycerol Lipase  $\alpha$  Inhibitors. *J. Med. Chem.* **58**, 9742–9753 (2015).

44. Kathuria, S. *et al.* Modulation of anxiety through blockade of anandamide hydrolysis. *Nat. Med.* **9**, 76–81 (2003).
45. Alexander, J. P. & Cravatt, B. F. Mechanism of Carbamate Inactivation of FAAH: Implications for the Design of Covalent Inhibitors and In Vivo Functional Probes for Enzymes. *Chem. Biol.* **12**, 1179–1187 (2005).
46. Zhang, D. *et al.* Fatty acid amide hydrolase inhibitors display broad selectivity and inhibit multiple carboxylesterases as off-targets. *Neuropharmacology* **52**, 1095–1105 (2007).
47. Clapper, J. R. *et al.* A Second Generation of Carbamate-Based Fatty Acid Amide Hydrolase Inhibitors with Improved Activity in vivo. *ChemMedChem* **4**, 1505–1513 (2009).
48. Clapper, J. R. *et al.* Anandamide suppresses pain initiation through a peripheral endocannabinoid mechanism. *Nat. Neurosci.* **13**, 1265–1270 (2010).
49. Greco, R. *et al.* Characterization of the peripheral FAAH inhibitor, URB937, in animal models of acute and chronic migraine. *Neurobiol. Dis.* **147**, 105157 (2021).
50. Li, W., Blankman, J. L. & Cravatt, B. F. A Functional Proteomic Strategy to Discover Inhibitors for Uncharacterized Hydrolases. *J. Am. Chem. Soc.* **129**, 9594–9595 (2007).
51. Long, J. Z. *et al.* Selective blockade of 2-arachidonoylglycerol hydrolysis produces cannabinoid behavioral effects. *Nat. Chem. Biol.* **5**, 37–44 (2009).
52. Long, J. Z., Nomura, D. K. & Cravatt, B. F. Characterization of Monoacylglycerol Lipase Inhibition Reveals Differences in Central and Peripheral Endocannabinoid Metabolism. *Chem. Biol.* **16**, 744–753 (2009).
53. Schlosburg, J. E. *et al.* Chronic monoacylglycerol lipase blockade causes functional antagonism of the endocannabinoid system. *Nat. Neurosci.* **13**, 1113–1119 (2010).
54. Chang, J. W. *et al.* Highly Selective Inhibitors of Monoacylglycerol Lipase Bearing a Reactive Group that Is Bioisosteric with Endocannabinoid Substrates. *Chem. Biol.* **19**, 579–588 (2012).
55. Chang, J. W., Coggnetta, A. B., Niphakis, M. J. & Cravatt, B. F. Proteome-Wide Reactivity Profiling Identifies Diverse Carbamate Chemotypes Tuned for Serine Hydrolase Inhibition. *ACS Chem. Biol.* **8**, 1590–1599 (2013).
56. Prokop, S. *et al.* PharmacostORM nanoscale pharmacology reveals cariprazine binding on Islands of Calleja granule cells. *Nat. Commun.* **12**, 6505 (2021).
57. Cisar, J. S. *et al.* Identification of ABX-1431, a Selective Inhibitor of Monoacylglycerol Lipase and Clinical Candidate for Treatment of Neurological Disorders. *J. Med. Chem.* **61**, 9062–9084 (2018).
58. Müller-Vahl, K. R. *et al.* Endocannabinoid Modulation Using Monoacylglycerol Lipase Inhibition in Tourette Syndrome: A Phase 1 Randomized, Placebo-Controlled Study. *Pharmacopsychiatry* **55**, 148–156 (2022).

59. Müller-Vahl, K. R. *et al.* Monoacylglycerol Lipase Inhibition in Tourette Syndrome: A 12-Week, Randomized, Controlled Study. *Mov. Disord.* **36**, 2413–2418 (2021).
60. McAllister, L. A. *et al.* Discovery of Trifluoromethyl Glycol Carbamates as Potent and Selective Covalent Monoacylglycerol Lipase (MAGL) Inhibitors for Treatment of Neuroinflammation. *J. Med. Chem.* **61**, 3008–3026 (2018).
61. Moore, S. A. *et al.* Identification of a high-affinity binding site involved in the transport of endocannabinoids. *Proc. Natl. Acad. Sci. U.S.A.* **102**, 17852–17857 (2005).
62. Alexander, J. P. & Cravatt, B. F. The Putative Endocannabinoid Transport Blocker LY2183240 Is a Potent Inhibitor of FAAH and Several Other Brain Serine Hydrolases. *J. Am. Chem. Soc.* **128**, 9699–9704 (2006).
63. Johnson, D. S. *et al.* Benzothiophene piperazine and piperidine urea inhibitors of fatty acid amide hydrolase (FAAH). *Bioorg. Med. Chem. Lett.* **19**, 2865–2869 (2009).
64. Janssen Pharmaceutica N.V. US7598249B2. (2009).
65. Pfizer Inc. WO2009127949. (2009).
66. Pfizer Inc. US 2010/0113465 A1. (2010).
67. Keith, J. M. *et al.* Preclinical Characterization of the FAAH Inhibitor JNJ-42165279. *ACS Med. Chem. Lett.* **6**, 1204–1208 (2015).
68. NCT01650597. *Clinicaltrial.gov*.
69. Postnov, A. *et al.* Fatty Acid Amide Hydrolase Inhibition by JNJ-42165279: A Multiple-Ascending Dose and a Positron Emission Tomography Study in Healthy Volunteers. *Clin. Transl. Sci.* **11**, 397–404 (2018).
70. Schmidt, M. E. *et al.* The effects of inhibition of fatty acid amide hydrolase (FAAH) by JNJ-42165279 in social anxiety disorder: a double-blind, randomized, placebo-controlled proof-of-concept study. *Neuropsychopharmacology* **46**, 1004–1010 (2021).
71. Huggins, J. P., Smart, T. S., Langman, S., Taylor, L. & Young, T. An efficient randomised, placebo-controlled clinical trial with the irreversible fatty acid amide hydrolase-1 inhibitor PF-04457845, which modulates endocannabinoids but fails to induce effective analgesia in patients with pain due to osteoarthritis of the knee. *Pain* **153**, 1837–1846 (2012).
72. D’Souza, D. C. *et al.* Efficacy and safety of a fatty acid amide hydrolase inhibitor (PF-04457845) in the treatment of cannabis withdrawal and dependence in men: a double-blind, placebo-controlled, parallel group, phase 2a single-site randomised controlled trial. *Lancet Psychiatry* **6**, 35–45 (2019).
73. Mayo, L. M. *et al.* Elevated Anandamide, Enhanced Recall of Fear Extinction, and Attenuated Stress Responses Following Inhibition of Fatty Acid Amide Hydrolase: A Randomized, Controlled Experimental Medicine Trial. *Biol. Psychiatry* **87**, 538–547 (2020).

74. Bonini, S. & Rasi, G. First-in-Human Clinical Trials — What We Can Learn from Tragic Failures. *N. Engl. J. Med.* **375**, 1788–1789 (2016).
75. van Esbroeck, A. C. M. *et al.* Activity-based protein profiling reveals off-target proteins of the FAAH inhibitor BIA 10-2474. *Science* **356**, 1084–1087 (2017).
76. Hsu, K.-L. *et al.* DAGL $\beta$  inhibition perturbs a lipid network involved in macrophage inflammatory responses. *Nat. Chem. Biol.* **8**, 999–1007 (2012).
77. van der Wel, T. *et al.* A natural substrate-based fluorescence assay for inhibitor screening on diacylglycerol lipase  $\alpha$ . *J. Lipid. Res.* **56**, 927–935 (2015).
78. Deng, H. *et al.* Triazole Ureas Act as Diacylglycerol Lipase Inhibitors and Prevent Fasting-Induced Refeeding. *J. Med. Chem.* **60**, 428–440 (2017).
79. Ogasawara, D. *et al.* Rapid and profound rewiring of brain lipid signaling networks by acute diacylglycerol lipase inhibition. *Proc. Natl. Acad. Sci. U.S.A.* **113**, 26–33 (2016).
80. Janssen, A. P. A. *et al.* Structure Kinetics Relationships and Molecular Dynamics Show Crucial Role for Heterocycle Leaving Group in Irreversible Diacylglycerol Lipase Inhibitors. *J. Med. Chem.* **62**, 7910–7922 (2019).
81. Hsu, K.-L. *et al.* Discovery and Optimization of Piperidyl-1,2,3-Triazole Ureas as Potent, Selective, and in Vivo-Active Inhibitors of  $\alpha/\beta$ -Hydrolase Domain Containing 6 (ABHD6). *J. Med. Chem.* **56**, 8270–8279 (2013).
82. Manterola, A. *et al.* Deregulation of the endocannabinoid system and therapeutic potential of ABHD6 blockade in the cuprizone model of demyelination. *Biochem. Pharmacol.* **157**, 189–201 (2018).
83. Manterola, A. *et al.* Re-examining the potential of targeting ABHD6 in multiple sclerosis: Efficacy of systemic and peripherally restricted inhibitors in experimental autoimmune encephalomyelitis. *Neuropharmacology* **141**, 181–191 (2018).
84. Appiah, K. K. *et al.* Identification of Small Molecules That Selectively Inhibit Diacylglycerol Lipase- $\alpha$  Activity. *SLAS Discov.* **19**, 595–605 (2014).
85. Janssen, F. J. *et al.* Discovery of Glycine Sulfonamides as Dual Inhibitors of sn -1-Diacylglycerol Lipase  $\alpha$  and  $\alpha/\beta$ -Hydrolase Domain 6. *J. Med. Chem.* **57**, 6610–6622 (2014).
86. Chupak, L. S. *et al.* Structure activity relationship studies on chemically non-reactive glycine sulfonamide inhibitors of diacylglycerol lipase. *Bioorg. Med. Chem.* **24**, 1455–1468 (2016).
87. Ogasawara, D. *et al.* Selective blockade of the lyso-PS lipase ABHD12 stimulates immune responses in vivo. *Nat. Chem. Biol.* **14**, 1099–1108 (2018).
88. Cognetta, A. B. *et al.* Selective *N*-Hydroxyhydantoin Carbamate Inhibitors of Mammalian Serine Hydrolases. *Chem. Biol.* **22**, 928–937 (2015).

89. Ogasawara, D. *et al.* Discovery and Optimization of Selective and in Vivo Active Inhibitors of the Lysophosphatidylserine Lipase  $\alpha/\beta$ -Hydrolase Domain-Containing 12 (ABHD12). *J. Med. Chem.* **62**, 1643–1656 (2019).
90. Kathman, S. G., Boshart, J., Jing, H. & Cravatt, B. F. Blockade of the Lysophosphatidylserine Lipase ABHD12 Potentiates Ferroptosis in Cancer Cells. *ACS Chem. Biol.* **15**, 871–877 (2020).
91. Zhou, J. *et al.* Structure–Activity Relationship Studies of  $\alpha$ -Ketoamides as Inhibitors of the Phospholipase A and Acyltransferase Enzyme Family. *J. Med. Chem.* **63**, 9340–9359 (2020).
92. Mock, E. D. *et al.* Discovery of a NAPE-PLD inhibitor that modulates emotional behavior in mice. *Nat. Chem. Biol.* **16**, 667–675 (2020).
93. Mock, E. D. *et al.* Structure–Activity Relationship Studies of Pyrimidine-4-Carboxamides as Inhibitors of N -Acylphosphatidylethanolamine Phospholipase D. *J. Med. Chem.* **64**, 481–515 (2021).
94. Pang, Z. *et al.* *In situ* identification of cellular drug targets in mammalian tissue. *Cell* **185**, 1793–1805 (2022).